International Journal on Advanced Science Engineering Information Technology

Vol.11 (2021) No. 2
ISSN: 2088-5334

Geochemical Analysis of Metal Minerals on Kuantan Singingi Regency, Riau Province as a Connection part of Bukit Barisan Mountain, West Sumatera, Indonesia

Husnul Kausarian[a,*], Ridwan Rahmanto[a], Adi Suryadi[a], Dewandra Bagus Eka Putra[a], Fitri Mairizki[a], Muhammad Zainuddin Lubis[b]

[a]*Department of Geological Engineering, Universitas Islam Riau, Jl. Kaharuddin Nasution 113, Pekanbaru, 28284, Indonesia*
[a]*Department of Geomatics Engineering, Politeknik Negeri Batam, Batam, Indonesia*
*Corresponding author: *husnulkausarian@eng.uir.ac.id*

***Abstract*— The research area is located in Muara Lembu Village, Singingi District, Kuantan Singingi Regency, Riau Province. Located at coordinates 0°25'40.85"S - 101°17'50.82"E and 0°26'45.50"S - 101°19'27.81"E. The research area's landform consists of slightly structural steep, structural sloping hills, and low denudational hills. The study area consists of a rock unit, which is claystone units indicated by a thin layer that formed metal minerals because of the erosional process in several places, which the erosion process transported to the research area. It is supported by thrust slip fault, resulting in gaps at the weak zone and eroded minerals filling and changing the claystone composition. At the same time, the oxidation process occurred in the research area. The geomorphology and stratigraphy analysis results show three types: Slightly Structural Steep, Structural Slooping Hills, and Low Denudational Hills. The results of Genesis and Potential Minerals in the study area consist of carrier rocks from the Claystone Unit. The deposition process can be called Sediment Genesis. The results of X-Ray Fluorescence (X-RF) and X-Ray Diffraction (X-RD) tests showed that the highest minerals are silica (SiO2) with metal mineral potentials such as pyrolusite (MnO_2), Muscovite ($H_2KAL_3Si_3O_{12}$), Graphite (C), Hematite (Fe_2O_3), Aluminum Oxide / Corundum (Al_2O_3), Manganese (Mn), Silver (Ag), and Titanium (Ti). This research showed the economic value in the form of iron and steel.**

***Keywords*— Muara Lembu; metal minerals; oxidation; X-Ray Fluorescence (XRF); X-Ray Diffraction (XRD).**

Manuscript received 15 May 2020; revised 15 Feb. 2021; accepted 25 Feb. 2021. Date of publication 30 Apr. 2021.

I. INTRODUCTION

Metal mineral resources, as one of the natural wealth owned by Indonesia [1] – [5], if it managed properly, will contribute to the economic development of the country. Metal minerals play an essential role in the life of modern technology nowadays. In 2014, Indonesia, according to the United States Geological Survey (USGS) ranked 6th as a rich country in mining resources [6]. If managed properly, it will make the mining sector contribute to Indonesia's gross domestic product (GDP), open up many jobs, and even create Indonesian mining professionals. One of the areas consist of abundant minerals (based on geological condition) [7] is in Muara Lembu Village, Kuantan Singingi Regency, Riau Province, which alines continuously to the Bukit Barisan Mountain, West Sumatera, Indonesia (Figure 1).

II. MATERIALS AND METHOD

A. Materials

1) Stratigraphy; members of Batusabak and shale tuhur formation (tits): Tuhur formation [8], [9] is the bedrock Based on its lithological. Tuhur formation's lithology are Batusabak, members of shale, Napalan shale, inserts shale, Radiolarite, a thin layer of metamorphosed greywacke, and a member of the Triassic Limestone.

2) Metal Mineral: Minerals that contain one type of metal or several metal associations are called metallic minerals [10], [11]. If the metal content is relatively large and chemically bound to other elements, it is called an ore mineral. Iron is the second most abundant metal on earth. The character of these iron deposits can be metal deposits that stand alone but often found associated with other metal minerals. Iron is sometimes present as a soil metal content (residual) but rarely has a high economic value. Economic iron deposits are Magnetite, Hematite, Limonite, and Siderite. Sometimes it can be in minerals: Pyrite, Pyrrhotite, Marcasite, and Chamosite [12] – [16].

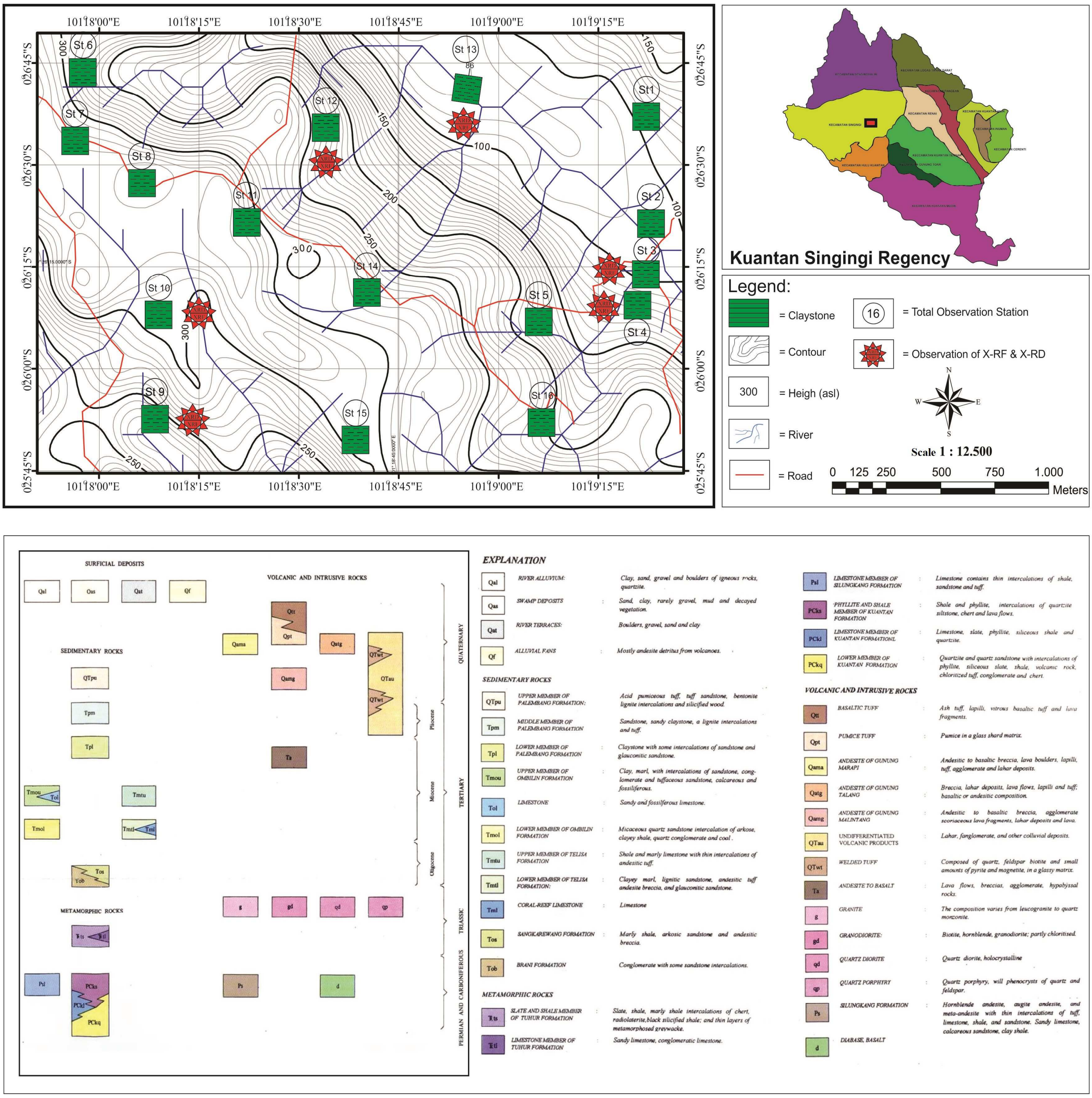

Fig. Map Location of Research Area and Stratigraphic Column of Regional Geological Map Solok Sheet [17].

A. Method

To recognize the rock, including lithology characteristics, rock structure of all rock outcrops in the mapping area, rock sampling is essential to be examined. As the second step, Geomorphological elements such as contour, the hills, elevations, slope, drainage, etc., are observed and calculated.

3) Geomorphological analysis: Geomorphology is defined as a study that describes landforms and processes and looks for the relationships between landforms and spatial arrangement processes [18]-[23]. The formation of an area's landform is the result of a geomorphological process caused by an endogenous and exogenous force.

4) Lithology analysis: The lithology analysis is used to determine the geological unit boundaries for each rock/formation [24]-[26].

5) X-Ray Fluorescence (X-RF) analysis: XRF is widely used to determine the elemental composition of material because this method is fast and does not damage the sample [27]-[30]. This method was chosen for application in the field and industry for material control.

6) *X-Ray Diffraction (X-RD) analysis:* XRD is used to determine the minerals contained in mining material and its associations [31]-[35].

III. Result and Discussion

A. Geomorphology and Stratigraphy

1) Unit of unit of slightly structural steep: This geomorphological unit is in the Northwest and Southeast parts of the study area, with a 35% distribution percentage in slightly structural areas. It has a 15-30% slope percentage of and with elevation 250 - 300 masl (Figure 2).

Fig. 2 Geomorphological unit of a slightly steep structural hill.

2) Unit of structural sloping hills: This geomorphological unit is in the Southwest part of the research area with a 45% distribution percentage found in areas with sloping slopes and has 7-15% of a slope with 100 - 200 masl elevation (Figure 3).

Fig. 3 Geomorphology unit of Structural Sloping Hills.

3) Unit of low denudational hills: This geomorphology unit is located in the Northeast area of research with a 20% percentage distribution, which found a low slope with a 07-15% slope with 50-100 masl of elevation (Figure 4).

Fig. 4 Geomorphology Unit of Low Denudational Hills.

Meanwhile, the study area's stratigraphy (Figure 5) consists of clay rock units with lithology consisting of shall-clay with Triassic age. The study area's regional correlation is the member of slate and shale rock from the Tuhur formation.

Age	Rock Unit	Lithology	Regional Correlation
Triassic	Clay Rock	Shale-Clay Rock	Members of slate and Shale of Tuhur Formation

Fig. 5 Stratigraphic Column of Research Area.

B. Genesis and Potential Minerals

1) Claystone unit: claystone occupied the whole of the research area (Figure 6). Claystone in the research area shows the characteristics of weathered with grayish-brown and fresh color with gray color. The rock has a clay grain with a closed container, so it is not carbonated with rather hard compactness and has no contact between rocks (Figure 7).

2) Sediment genesis of metal minerals: According to observation, calculation, and analysis, metal minerals can be formed and found due to erosion in several places that occur due to weathering of the landform (Figure 8). The erosion is transported to the research area and supported by the presence of metal minerals. A fault that increases the opening of gaps in the weak zone and the eroded minerals enter then changes the composition of claystone minerals so that in the research area, metal minerals can be found. Furthermore, after the eroded minerals come and change the minerals' structure in the clay, then in an oxidation process, this oxidation process is common in weathering, namely iron oxidation.

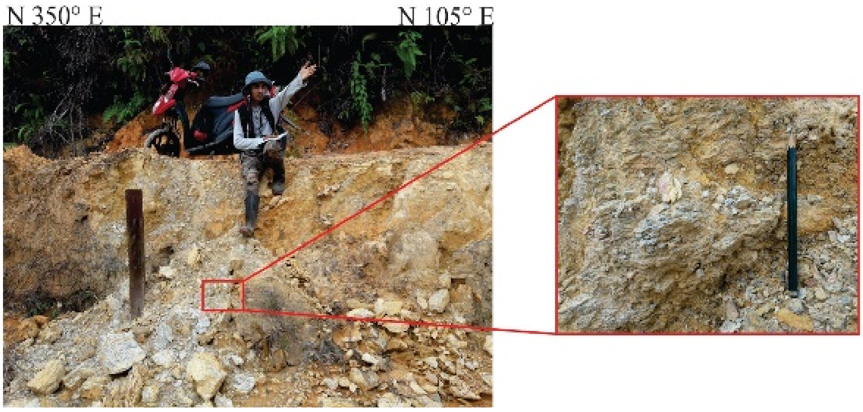

Fig. 6 Claystone Unit in the Research Area.

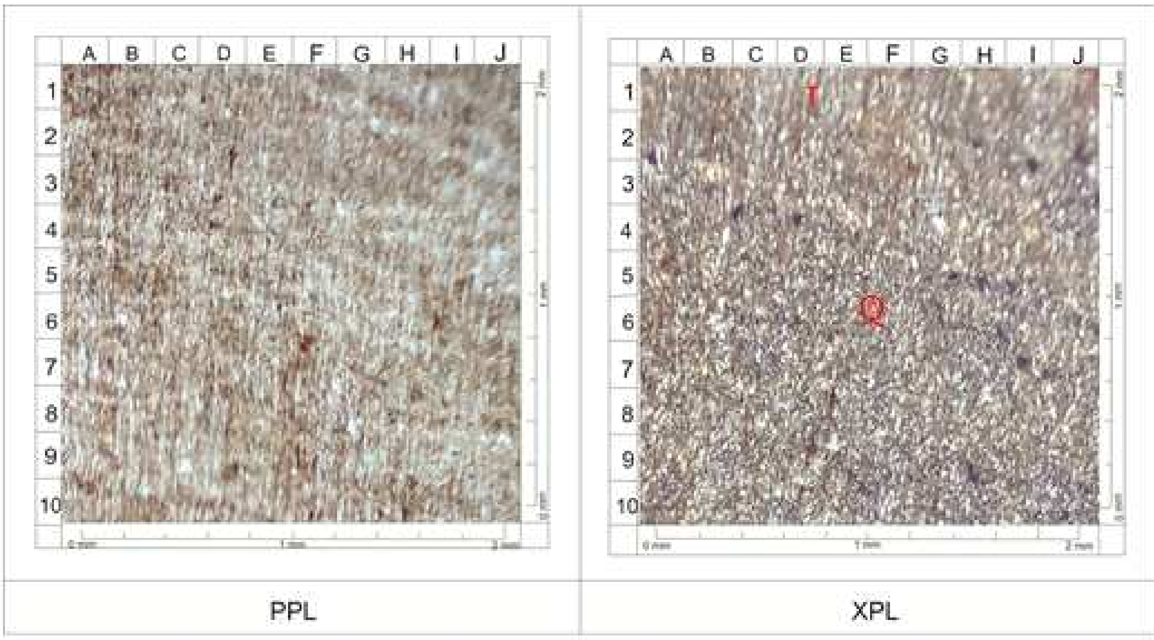

Fig. 7 The Appearance of Claystone Thin Section.

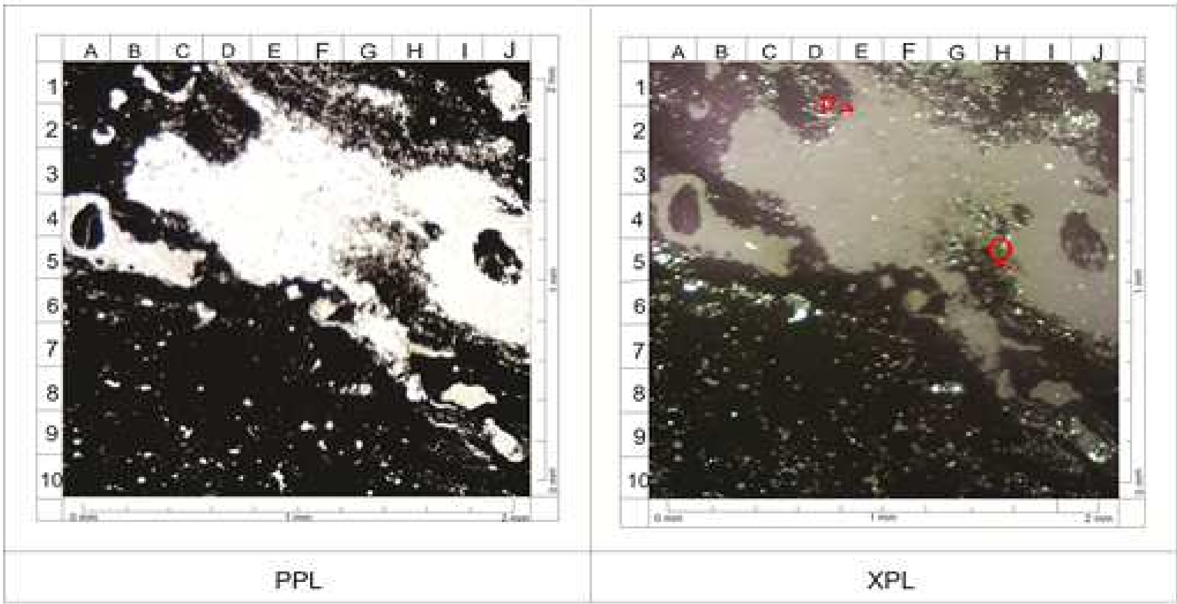

Fig. 8 The appearance of metal minerals thin section shows the erosion process has occurred to this sample.

3) X-Ray Diffraction (X-RD) result analysis: The potential area with a high composition of metal minerals has been identified and measured with six (6) samples (for sample distribution, see Figure 1). From Station 03, it can be seen the Pyrolusite mineral deposit (MnO_2) is the lowest peak value while the Silica mineral deposit (SiO_2) is the highest peak value (Figure 9).

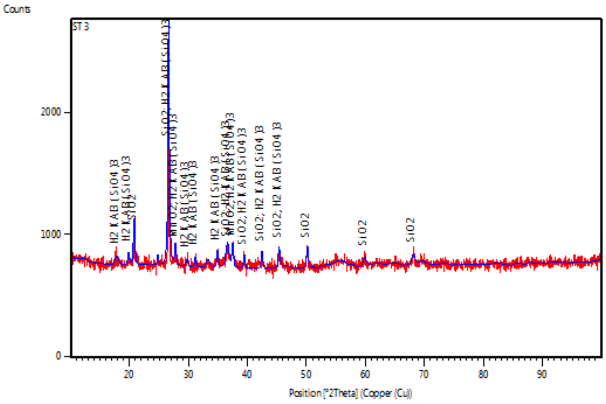

Fig. 9 X-Ray Diffraction Graph from Sample on Location 03.

From Station 04, it can be seen that Muscovite ($H_2KAL_3Si_3O_{12}$) is the lowest peak value, while Graphite mineral deposit (C) is the highest peak value (Figure 10).

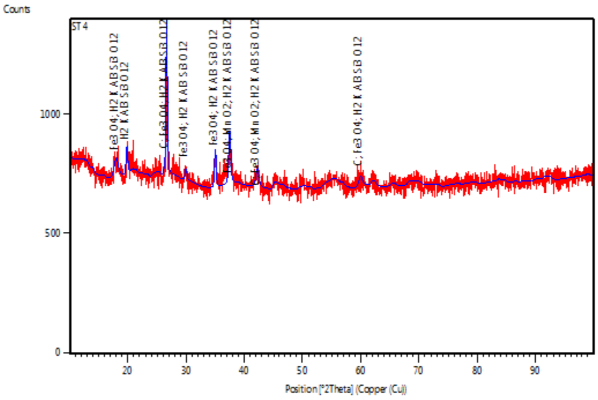

Fig. 10 X-Ray Diffraction Graph from Sample on Location 04.

From Station 09, it can be seen that Muscovite ($H_2KAL_3Si_3O_{12}$) is the lowest peak value, while the Silica (SiO_2) mineral deposit is the highest peak value (Figure 11). From Station 10, it can be seen Pyrolusite (MnO_2) is the lowest peak value while the silica mineral deposit (SiO2) is the highest peak value (Figure 12). From Station 12, it can be seen that Muscovite mineral deposit ($H_2KAL_3Si_3O_{12}$) is the lowest peak value, while silica mineral deposit (SiO_2) is the highest peak value (Figure 13). From Station 13, it can be seen that Muscovite mineral deposit ($H_2KAL_3Si_3O_{12}$) is the lowest peak value, while Silica (SiO_2) is the highest peak value (Figure 14).

X-Ray Fluorescence (X-RF) result analysis: Based on data from the results of geochemical analysis (XRF) at stations 03, 04, 09, 10, 12, and 13, we obtained several types of metal mineral deposits from the largest to the smallest in the study area (See Figure 1 to see the sampling locations).

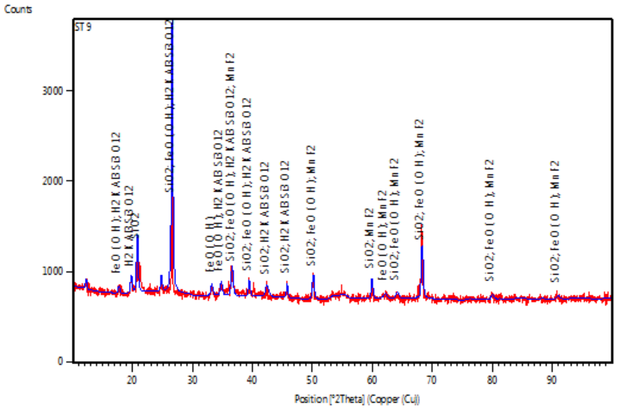

Fig. 11 X-Ray Diffraction Graph from Sample on Location 09.

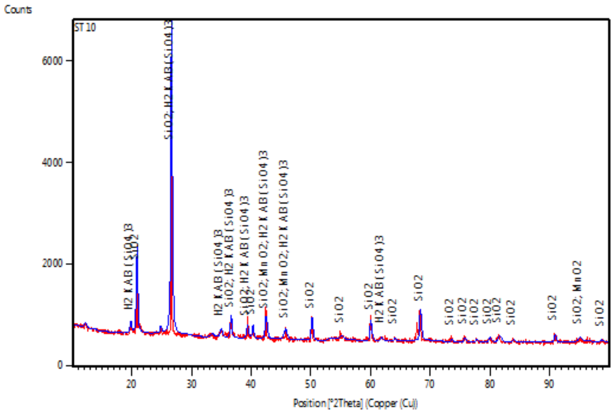

Fig. 12 X-Ray Diffraction Graph from Sample on Location 10.

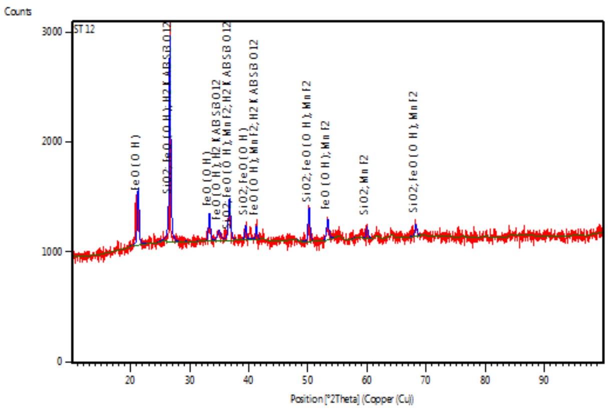

Fig. 13 X-Ray Diffraction Graph from Sample on Location 12.

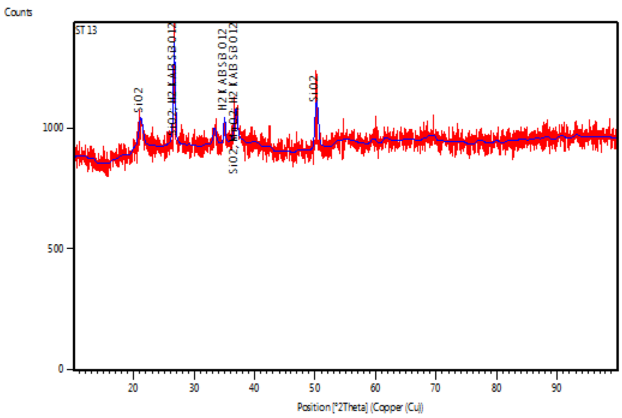

Fig. 14 X-Ray Diffraction Graph from Sample on Location 13.

Hematite (Fe_2O_3) mineral deposits resulted from the sedimentary rock formation, which was found in clay rocks in this research area. These mineral deposits scattered in the northern part of the geomorphological unit of a rather steep structural hill with a percentage distribution of 45% and an average value of weight percent that is 22,674% (Figure 15).

Aluminum Oxide/Corundum (Al_2O_3) mineral deposits resulted from the elements magnetite, hematite, and spinel in the study area and found in claystone. These mineral deposits are scattered in the Southwest part in the rather steep structural geomorphological hills with a percentage distribution of 45% and an average value of percent weight that is 16,688% (Figure 16).

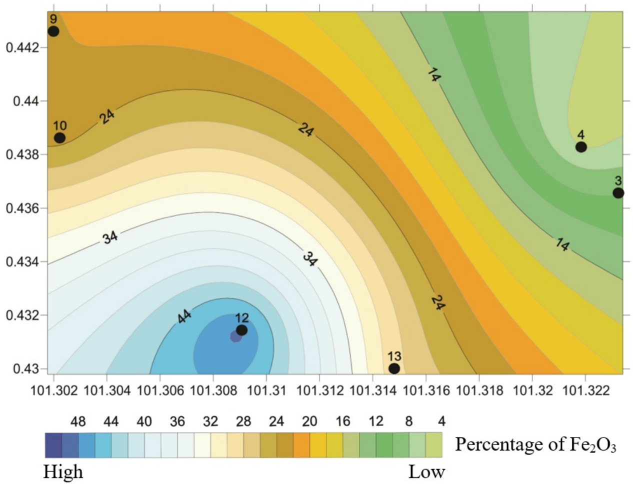

Fig. 15 Hematite (Fe_2O_3) Composition and Percentage from Research Area.

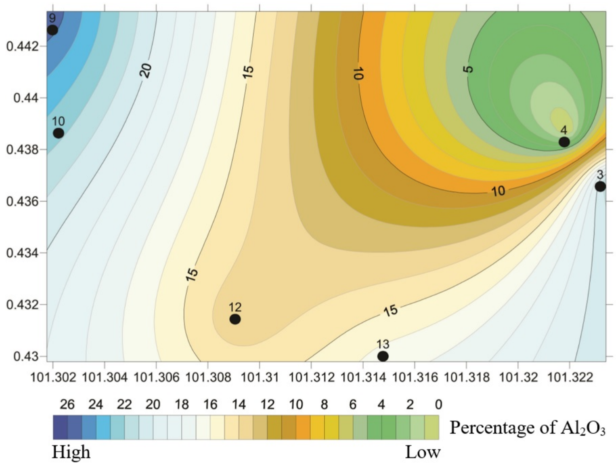

Fig. 16 Aluminum Oxide/Corundum (Al_2O_3) Composition and Percentage from Research Area.

Manganese (Mn) mineral deposits result from iron ore and mineral changes in the study area in claystone. These mineral deposits are scattered in the eastern part of the geomorphological unit of a rather steep structural hill with a percentage distribution of 35% and an average value percent by weight is 11,445% (Figure 17).

Silver (Ag) mineral deposits result from natural formation and other metal minerals such as Nickel and Tin, which are found in the study area in claystone. These mineral deposits are scattered in the northern part of the relatively steep structural hills' structural geomorphology with a percentage distribution of 15% and an average value of percent weight that is 0.752% (Figure 18).

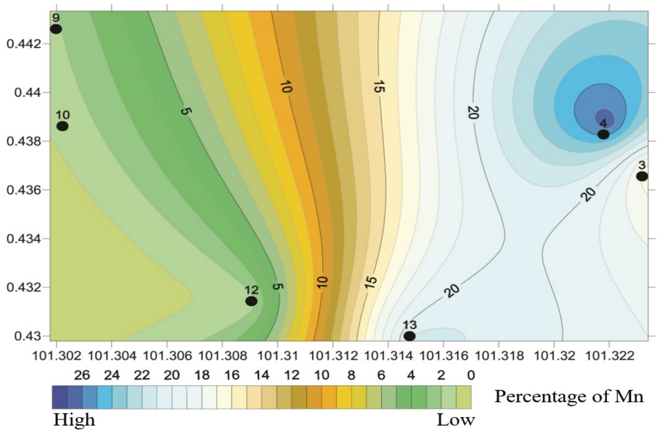

Fig. 17 Manganese (Mn) Composition and Percentage from Research Area.

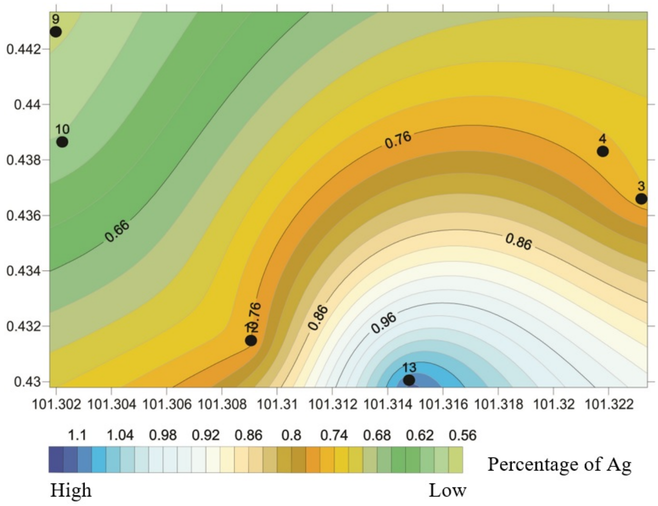

Fig. 18 Silver (Ag) Composition and Percentage from Research Area.

Titanium (Ti) mineral deposits can be associated with Magnetite, Hematite, Spatite, and quartz, which are found in the study area in claystone. These mineral deposits are scattered in the Southwest part in the rather steep structural geomorphological hills with a percentage distribution of 10% and an average value of percent weight that is 0.283% (Figure 19).

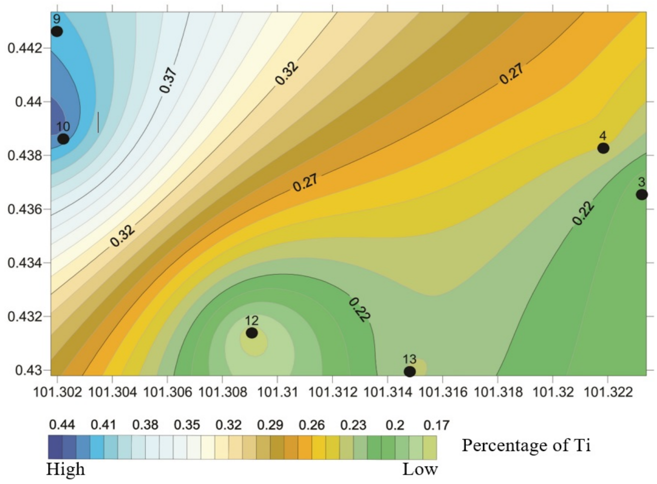

Fig. 19 Titanium (Ti) Composition and Percentage from Research Area.

C. Potential and Utilization of Metal Mineral Deposits

The potential of metal mineral deposits in the research area is quite good because there are several variations of types of metallic mineral deposits. If further research is carried out on a large scale, it will support creating the exploration and exploitation process. Metal mineral deposits in the research area are dominated by Hematite, Manganese, Titanium, and other deposits, which can provide economic value because they are widely used as materials in the manufacture of iron and steel and other industries.

IV. Conclusion

Genesis and topography control the deposition of metal minerals in the research area as the deposition environment. Stratigraphically, the study area is composed of a single rock unit, the claystone unit, which is pre-tertiary, with lithology characteristics of flake clay. The genesis and origins of metal mineral deposits in the research area are due to the claystone transformation mineral composition and the oxidation process. Metal mineral deposits in the research area are classified based on genesis or the mineral deposit formation origin. Based on geochemical analysis results (XRF and XRD) obtained various types of mineral deposits, including Hematite, Manganese, Silver, Titanium, Graphite, Goethite deposits.

Acknowledgment

The authors are grateful to the Universitas Islam Riau as the primary foundation for this research, especially for the Engineering Geological Program, Faculty of Engineering. Special thanks are also addressed to the Government of Riau Province to support this research's secondary data.

References

[1] Van der Ploeg, F., “Natural resources: curse or blessing?”. *Journal of Economic literature*, Vol. 49(2), pp.366-420. 2011.

[2] Vanitha, M., Camellia, P. and Balasubramanian, N., “Augmentation of graphite purity from mineral resources and enhancing% graphitization using microwave irradiation: XRD and Raman studies”. *Diamond and Related Materials*, Vol. 88, pp.129-136. 2018.

[3] Arndt, N.T., Fontboté, L., Hedenquist, J.W., Kesler, S.E., Thompson, J.F. and Wood, D.G., “Future global mineral resources”. *Geochemical Perspectives*, Vol. 6(1), pp.1-171. 2017.

[4] Christmann, P., “Towards a more equitable use of mineral resources”. *Natural Resources Research*, Vol. 27(2), pp.159-177. 2018.

[5] Maulana, A., Sanematsu, K. and Sakakibara, M., “An Overview on the Possibility of Scandium and REE Occurrence in Sulawesi, Indonesia”. *Indonesian Journal on Geoscience*, Vol. 3(2), pp.139-147. 2016.

[6] Kurniawan, R. and Managi, S., “Economic growth and sustainable development in Indonesia: an assessment”. *Bulletin of Indonesian Economic Studies*, Vol. 54(3), pp.339-361. 2018.

[7] Kausarian, H., Sumantyo, S., Tetuko, J., Kuze, H., Karya, D. and Panggabean, G.F., “Silica Sand Identification using ALOS PALSAR Full Polarimetry on The Northern Coastline of Rupat Island, Indonesia”. *International Journal on Advanced Science, Engineering and Information Technology*, Vol. 6(5), pp.568-573. 2016.

[8] Putra, A.M., “First evidence of Middle to Late Triassic radiolarians in the Garba mountains, South Sumatra, Indonesia”. *Island Arc*, Vol. 28(3), p.e12298. 2019.

[9] Kausarian, H., Sri Sumantyo, J.T., Kuze, H., Aminuddin, J. and Waqar, M.M., “Analysis of polarimetric decomposition, backscattering coefficient, and sample properties for identification and layer thickness estimation of silica sand distribution using L-band synthetic aperture radar”. *Canadian Journal of Remote Sensing*, Vol. 43(2), pp.95-108. 2017.

[10] Azapagic, A., “Developing a framework for sustainable development indicators for the mining and minerals industry”. *Journal of cleaner production*, *12*(6), pp.639-662. 2004.

[11] Bateman, A.M. and Jensen, M.L., “*Economic mineral deposits”* (Vol. 259). New York: Wiley. 1950.

[12] Mukherjee, S., “Mineral Deposits and Their Characteristics”. In *Applied Mineralogy* (pp. 262-280). Springer, Dordrecht. 2011.

[13] Chen, F., Deng, J., Wang, Q., Huizenga, J.M., Li, G. and Gu, Y., “LA-ICP-MS trace element analysis of magnetite and pyrite from the Hetaoping Fe-Zn-Pb skarn deposit in Baoshan block, SW China: implications for ore-forming processes”. *Ore Geology Reviews*, p.103309. 2020.

[14] Thibault, Y., McEvoy, J.G. and Beauchemin, S., “Iron and sulphur management options during Ni recovery from (bio) leaching of pyrrhotite tailings, Part 1: Mechanisms of low-temperature transformation from goethite and jarosite to magnetic spinel. *Minerals Engineering*, Vol. 150, p.106265. 2020.

[15] Wu, Y.F., Li, J.W., Evans, K., Koenig, A.E., Li, Z.K., O’Brien, H., Lahaye, Y., Rempel, K., Hu, S.Y., Zhang, Z.P. and Yu, J.P., “Ore-forming processes of the Daqiao Epizonal Orogenic gold deposit, West Qinling Orogen, China: Constraints from textures, trace elements, and sulfur isotopes of pyrite and marcasite, and Raman spectroscopy of carbonaceous material”. *Economic Geology*, Vol. 113(5), pp.1093-1132. 2018.

[16] Brusnitsyn, A.I., Kuleshov, V.N., Perova, E.N. and Zaitsev, A.N., “Ferromanganese carbonate metasediments of the Sob area, Polar Urals: Bedding conditions, composition, and genesis”. *Lithology and Mineral Resources*, Vol. 52(3), pp.192-213. 2017.

[17] Silitonga, P.H. and Kastowo, D., “Geological Map of the Solok Quadrangle, Sumatra (Quadrangle 0815) Scale 1: 250,000”. *Geological Research and Development Centre Bandung,*. 1995.

[18] Wheaton, J.M., Fryirs, K.A., Brierley, G., Bangen, S.G., Bouwes, N. and O'Brien, G., “Geomorphic mapping and taxonomy of fluvial landforms”. *Geomorphology*, Vol. 248, pp.273-295. 2015.

[19] Huggett, R., “*Fundamentals of geomorphology”*. Routledge. 2007.

[20] Chorley, R.J. ed., “*Spatial analysis in geomorphology”*. Routledge. 2019.

[21] Martínez-Graña, A.M., Silva, P.G., Goy, J.L., Elez, J., Valdés, V. and Zazo, C., “Geomorphology applied to landscape analysis for planning and management of natural spaces. Case study: Las Batuecas-S. de Francia and Quilamas natural parks,(Salamanca, Spain)”. *Science of the Total Environment*, 2017. Vol. 584, pp.175-188. 2017.

[22] Singh, S., Guha, A., Seshadri, K. and Kumar, K.V., “Earth observation-based approach for delineating geomorphology-guided geoenvironmental zones and its utility in regional planning: an analysis in parts of Bengal Basin, West Bengal, India”. *Environmental Earth Sciences*, *76*(3), p.109. 2017.

[23] Koohafkan, M.C. and Gibson, S., “Geomorphic trajectory and landform analysis using graph theory: A panel data approach to quantitative geomorphology”. *Progress in Physical Geography: Earth and Environment*, *42*(6), pp.679-696. 2018.

[24] Gunsallus, K.T. and Kulhawy, F.H., “A comparative evaluation of rock strength measures”. In *International Journal of Rock Mechanics and Mining Sciences & Geomechanics Abstracts,* (Vol. 21, No. 5, pp. 233-248). Pergamon. 1984.

[25] Zhong, Y.H. and Li, R., “Application of principal component analysis and least square support vector machine to lithology identification”. *Well Logging Technology*, *33*(5), pp.425-429. 2009.

[26] Xianzheng, Z.H.A.O., Xiugang, P.U., Wenzhong, H.A.N., Lihong, Z.H.O.U., Zhannan, S.H.I., Shiyue, C.H.E.N. and Dunqing, X.I.A.O., “A new method for lithology identification of fine grained deposits and reservoir sweet spot analysis: A case study of Kong 2 Member in Cangdong sag, Bohai Bay Basin, China”. *Petroleum Exploration and Development*, Vol. 44(4), pp.524-534. 2017.

[27] Zang, A., Stephansson, O., Heidbach, O. and Janouschkowetz, S., “World stress map database as a resource for rock mechanics and rock engineering”. *Geotechnical and Geological Engineering*, Vol. 30(3), pp.625-646. 2012.

[28] Odoh, C.M., Garba, N.N., Nasiru, R., Saleh, M.A. and Ezekiel, Y.A., “The Effect of Geological Formations on Natural Radioactivity and Radiological Hazards in the Northern Zamfara State, Nigeria”. *Modern Physics*, *5*(1), pp.18-23. 2018.

[29] Osuji, O.S. and Akinwamide, J.T., "Physico-Chemical Properties of Lateritic Soils in Ado-Ekiti, South Western Nigeria". *Universal Journal of Environmental Research & Technology*, Vol. 7(1). 2018.

[30] Cawthorn, R.G., Latypov, R., Klemd, R. and Vuthuza, A., "Origin of discordant ultramafic pegmatites in the Bushveld Complex from externally-derived magmas". *South African Journal of Geology 2018*, *121*(3), pp.287-310. 2018.

[31] Brodaric, B., Gahegan, M. and Harrap, R., "The art and science of mapping: computing geological categories from field data". *Computers & Geosciences*, Vol. 30(7), pp.719-740. 2004.

[32] Moioli, P. and Seccaroni, C., "Analysis of art objects using a portable x-ray fluorescence spectrometer". *X-Ray Spectrometry: An International Journal*, *29*(1), pp.48-52. 2000.

[33] Kausarian, H., Choanji, T., Karya, D., Kadir, E.A. and Suryadi, A., "Geological Mapping of Silica Sand Distribution on the Muda Island and Ketam Island, Estuary of Kampar River, Indonesia". In *Proceedings of the Second International Conference on the Future of ASEAN (ICoFA) 2017–Volume 2* (pp. 973-982). Springer, Singapore. 2018.

[34] Hassellöv, M., Lyvén, B., Bengtsson, H., Jansen, R., Turner, D.R. and Beckett, R., "Particle size distributions of clay-rich sediments and pure clay minerals: a comparison of grain size analysis with sedimentation field-flow fractionation". *Aquatic Geochemistry*, Vol. 7(2), pp.155-171. 2001.

[35] Emery, X., "Conditioning simulations of Gaussian random fields by ordinary kriging". *Mathematical Geology*, Vol. 39(6), pp.607-623. 2007.